The Heavy Chain of Conventional Kinesin Interacts with the SNARE Proteins SNAP25 and SNAP23[†]

Russell J. Diefenbach,* Eve Diefenbach, Mark W. Douglas, and Anthony L. Cunningham

Centre For Virus Research, Westmead Millennium Institute, Westmead Hospital and The University of Sydney, Westmead, NSW 2145, Australia

Received July 9, 2002; Revised Manuscript Received September 6, 2002

ABSTRACT: Recent studies on the conventional motor protein kinesin have identified a putative cargo-binding domain (residues 827−906) within the heavy chain. To identify possible cargo proteins which bind to this kinesin domain, we employed a yeast two-hybrid assay. A human brain cDNA library was screened, using as bait residues 814−963 of human ubiquitous kinesin heavy chain. This screen initially identified synaptosome-associated protein of 25 kDa (SNAP25) as a kinesin-binding protein. Subsequently, synaptosome-associated protein of 23 kDa (SNAP23), the nonneuronal homologue of SNAP25, was also confirmed to interact with kinesin. The sites of interaction, determined from in vivo and in vitro assays, are the N-terminus of SNAP25 (residues 1−84) and the cargo-binding domain of kinesin heavy chain (residues 814−907). Both regions are composed almost entirely of heptad repeats, suggesting the interaction between heavy chain and SNAP25 is that of a coiled-coil. The observation that SNAP23 also binds to residues 814−907 of heavy chain would indicate that the minimal kinesin-binding domain of SNAP23 and SNAP25 is most likely residues 45−84 (SNAP25 numbering), a heptad-repeat region in both proteins. The major binding site for kinesin light chain in kinesin heavy chain was mapped to residues 789−813 at the C-terminal end of the heavy chain stalk domain. Weak binding of light chain was also detected at the N-terminus of the heavy chain tail domain (residues 814−854). In support of separate binding sites on heavy chain for light chain and SNAPs, a complex of heavy and light chains was observed to interact with SNAP25 and SNAP23.

The superfamily of kinesin molecular motor proteins together with cytoplasmic dynein are responsible for microtubule-dependent transport of cargo in eukaryotic cells (*1*, *2*). Conventional kinesin, the first member of the kinesin superfamily to be discovered (*3*, *4*), is a tetrameric protein consisting of two heavy chains and two light chains (*5*). The mammalian genome contains at least three conventional kinesin heavy chain (KHC) genes (KIF5A, KIF5B, and KIF5C) (*6*−*9*) and three kinesin light chain (KLC) genes (KLC1, KLC2, and KLC3) (*10*). Both KLC1 and KLC2 have been shown to interact with both KIF5A and KIF5B (*10*). The interaction between KHC and KLC is dependent on heptad-repeat regions in the N-terminal half of KLC (*11*, *12*) and the C-terminal end of the stalk domain of KHC (*12*, *13*).

It is becoming apparent that both KHC and KLC are capable of interacting with multiple cargo proteins through specific domains. Several cargo proteins have now been identified which bind to the C-terminal tetratricopeptide repeat (TPR) region of KLC (*14*). These cargo proteins include: JIP1, JIP2, and JIP3 (c-Jun amino-terminal kinase-interacting proteins) (*15*); *sunday driver* (JIP homologue in *Drosophila*) (*16*); and amyloid precursor protein (*17*, *18*). In addition, kinesin-dependent movement of vaccinia virus appears to be dependent on the TPRs of KLC (*19*). Studies with *Neurospora* conventional kinesin, which lacks a light chain, have demonstrated the presence of a cargo-binding region in the C-terminal heptad-repeat region of the heavy chain tail domain (*20*, *21*). Previous studies had implicated the C-terminal tail of KHC as having a direct role in binding of membranous cargo (*22*, *23*). Several proteins have now been shown to directly bind to the KHC tail domain including kinectin (*24*), Ran-binding protein 2 (RanBP2) (*25*), and the Herpes simplex viral protein US11 (*26*). In the case of both kinectin and US11, this interaction has been mapped to the predicted heptad-repeat cargo-binding region of KHC.

In this study we have further addressed the role of the KHC tail domain in transport of cargo in an attempt to shed more light on basic cellular transport processes and their link to disease processes, particularly neurodegenerative diseases. We conducted a yeast two-hybrid screen using conventional human ubiquitous (u) KHC (KIF5B) as bait to screen a human brain cDNA library. A new KHC-interacting protein was identified, namely, a synaptosome-associated protein of 25 kDa (SNAP25). In addition, a synaptosome-associated protein of 23 kDa (SNAP23), the ubiquitously expressed homologue of SNAP25, was also shown to directly interact with uKHC. The nature of the interaction was specific and likely to be an α-helical coiled-coil as the interaction was

[†] This work was supported by an Australian National Health and Medical Research Council grant to A.L.C. and R.J.D (No. 107374).

* Corresponding author. Phone: 61-2-9845-9111. Facsimile: 61-2-9845-9103. E-mail: russell_diefenbach@wmi.usyd.edu.au.

[1] Abbreviations: SNAP25 or SNAP23, synaptosome-associated protein of 25 or 23 kDa; SNARE, soluble *N*-ethylmaleimide-sensitive attachment protein receptor; t-SNARE, target membrane SNARE; KLC, kinesin light chain; KHC, kinesin heavy chain; uKHC, ubiquitous KHC; DIC, dynein intermediate chain; DLC, dynein light chain; TPR, tetratricopeptide repeat; GST, glutathione-*S*-transferase; His, oligohistidine; SD, synthetic dropout,; HA, hemagglutinin; GFP, green fluorescent protein; VAMP, vesicle-associated membrane protein.

10.1021/bi026417u CCC: $22.00
Published on Web 11/13/2002

shown to be mediated via heptad repeats in the tail domain of uKHC and the N-terminus of SNAP25.

MATERIAL AND METHODS

Expression Constructs. For yeast two-hybrid screen and binding assay, fragments of human uKHC and KLC were generated by PCR using Vent DNA polymerase (New England Biolabs) and inserted in frame with the LexA DNA-binding domain of displayBAIT vector (Display Systems Biotech). Amino acid residues 1−554 was amplified from plasmid pXPE, which contains the entire uKHC cDNA inserted into the *Xma*I and *Eco*RI sites of pSP72 vector (Promega), and was kindly provided by Dr Ron Vale (Howard Hughes Medical Institute, UCSF). Residues 555−813, 814−963, 555−866, 867−963, 814−907, and 908−963 were amplified from plasmid pET-28a/uKHC555−963 (*13*). Amino acid residues 4−199 and 200−569 of human KLC were amplified from plasmid pET-28a/KLC (*13*). Each PCR fragment was inserted into the *Eco*RI site of displayBAIT, except KHC(814−963) which was inserted into *Eco*RI- and *Bam*HI-digested displayBAIT and KHC(867−963) which was inserted into *Eco*RI- and *Xho*I-digested displayBAIT. Both PCR fragments of KLC were also inserted into the *Eco*RI site of displayTARGET (Display Systems Biotech) in frame with the B42 DNA-activation domain, while KHC(814−963) was inserted into *Eco*RI- and *Xho*I-digested displayTARGET. Fragments of human SNAP25 were amplified from full-length SNAP25 in displayTARGET vector obtained in this study. Fragments 1−84 and 85−206 were inserted into the *Eco*R*I* site of displayTARGET. Full-length SNAP25 was also excised from displayTARGET and inserted into *Eco*RI- and *Xho*I-digested displayBAIT. Full-length human SNAP23A inserted into the *Eco*RI and *Xho*I sites of vector pGEX4T-1 (*27*) was kindly provided by Dr Paul Roche (NCI, NIH). SNAP23 was excised from pGEX4T-1 and inserted into *Eco*RI- and *Xho*I-digested displayBAIT and displayTARGET vectors.

The cDNA for full-length human dynein intermediate chain (DIC)-1c in pBluescript (*28*) was kindly provided by Dr Lap-Chee Tsui (Department of Genetics, University of Toronto). The full-length cDNAs for human dynein light chains (DLCs) RP3, TcTex1, and LC8, along with human KIF3 accessory protein, KAP3B, were amplified from the same human brain cDNA library in displayTARGET as used for the library screen with KHC bait as detailed below. All PCR products were subsequently inserted into *Eco*RI- and *Xho*I-digested displayBAIT and displayTARGET except DIC which was cloned into *Eco*RI-digested vectors.

For in vitro binding studies, uKHC fragments were tagged at the N-terminus with a oligohistidine (His) tag. Fragments 1−554 and 814−963 were generated as above and inserted into *Bam*HI- and *Eco*RI-digested or *Bam*HI-digested pET-28a vector (Novagen), respectively. Fragments 876−963, 555−788, and 789−963 were generated by PCR and inserted into either *Hind*III-, *Bam*HI/*Eco*RI-, or *Bam*HI-digested pET-28a, respectively. Fragments 555−813, 555−772, 771−963, and 771−876 in pET-28a have been described previously (*13*). Glutathione-*S*-transferase (GST) fusion constructs of SNAP25 included full-length (1−206) along with fragments 1−84 and 85−206. The fragments were amplified as described above and inserted into *Bam*HI- and *Eco*RI-digested pGEX-2T (Amersham Pharmacia Biotech). Human KLC fragment 4−569 in pET-28a (minus His tag) and uKHC fragment 555−963 in pGEX-2T (kindly provided by Dr Ron Vale) have been described previously (*13*). All PCR amplified fragments were confirmed to be correct by sequencing.

Yeast Two-Hybrid Screen. The displayGREEN−BASIC two-hybrid system (Display Systems Biotech) was used according to the manufacturer's protocols. A human brain cDNA library fused to the activation domain of the displayTARGET vector was screened with the kinesin bait (uKHC814−963) fused to the DNA-binding domain of vector displayBAIT. In this system displayBAIT is equivalent to pLexA (Clontech), and displayTARGET is equivalent to pB42AD (Clontech). Yeast strain displayYEAST-H (Display Systems Biotech), which has the same genotype as EGY48 (Clontech), was initially co-transformed with kinesin bait and displayREPORTER vector (Display Systems Biotech). Yeast containing bait and reporter plasmids were then transformed with the cDNA library. Both small-scale and library transformation procedures were based on the lithium acetate method (Clontech Matchmaker LexA Two-Hybrid Protocol #PT3040-1). The transformants were assayed initially for expression of the *LEU2* reporter gene by plating on synthetic dropout (SD) minimal medium containing galactose/raffinose as the sole carbon source and deficient in histidine, leucine, uracil, and tryptophan, (SD/Gal/Raf/−His/−Leu/−Ura/−Trp). Putative positive colonies which grew on the selective medium were assayed for green fluorescent protein (GFP) expression from the displayREPORTER vector. Plates were exposed to UV light (365 nm), and colonies which displayed green fluorescence were marked for further analysis. False positives were then eliminated by testing Leu^+/GFP^+ colonies for growth on SD/dextrose/−His/−Leu/−Ura/−Trp. Only colonies which grew on SD/Gal/Raf/−His/−Leu/−Ura/−Trp and not on SD/dextrose/−His/−Leu/−Ura/−Trp and expressed GFP were potentially true positives.

Plasmid DNA was isolated from positive yeast colonies and transformed into *Escherichia coli* strain KC8 (Clontech). Bacteria transformed with the displayTARGET vector containing library cDNA were selected by plating on M9 minimal medium supplemented with an amino acid mixture lacking tryptophan. Plasmid DNA was isolated from these colonies, and the cDNA insert in displayTARGET was then sequenced and submitted to a BLAST search (http://www.ncbi.nlm.nih.gov:80/BLAST) to identify proteins that interacted with the kinesin bait.

Yeast Two-Hybrid Binding Studies. The yeast two-hybrid system was used to map the interacting domains of uKHC bait and SNAP25 identified in the initial two-hybrid screen. The protocols and constructs are described above except displayREPORTER was substituted with plasmid pSH18-34 (Invitrogen) that contains the *lacZ* reporter gene. Transformants on SD/Dextrose/−His/−Ura/−Trp agar plates were patched onto the same media as well as onto SD/Gal/Raf/−His/−Leu/−Ura/−Trp agar plates containing X-gal and BU salts (Clontech yeast protocols handbook #PT3024−1). At least 13 colonies were replica plated for each bait/target construct combination. Positive interactions on SD/Gal/Raf/−His/−Leu/−Ura/−Trp gave rise to blue growth as a result of activation of both *LEU2* and *lacZ* reporter genes. For determination of both β-galactosidase activity (Pierce Yeast β-galactosidase kit) and protein expression (Clontech yeast

protocols handbook #PT3024-1), patched colonies from SD/Dextrose/−His/−Ura/−Trp were used to inoculate SD/Gal/Raf/−His/−Ura/−Trp liquid media. At least three colony patches were picked for quantitative β-galactosidase activity determination.

In Vitro Binding Studies. The GST-fusion tag constructs were expressed in *E. coli* strain BL21. Protein expression was induced with 0.1 mM isopropyl-β-D-thiogalactoside for 3 h at 37 °C. The His-tag fusion and untagged KLC constructs were expressed and, along with the GST constructs, were harvested and lysed as previously described (*13*). The exception was that the lysis buffer was phosphate-buffered saline, pH 7.2, 5 mM dithiothreitol, 0.1% (v/v) Triton X-100, 5 ug/mL leupeptin and 1 mM PMFS. Soluble bacterial lysates (1 mL) containing GST fusion proteins were incubated with 50 ul of glutathione−sepharose beads (Amersham Pharmacia Biotech) for 4 h with rocking at 4 °C. The beads were washed three times with lysis buffer (minus protease inhibitors) before addition of soluble bacterial lysates (1 mL) containing His-tag fusion (or untagged KLC) proteins. Beads were incubated overnight at 4 °C with rocking before washing five times as described above. Protein complexes were then eluted using 1 bed volume of elution buffer (50 mM Tris−HCl, pH 8.0, 10 mM reduced glutathione) with rocking at 4 °C for 2 h. Batch binding experiments with His-tagged KHC fragments and untagged KLC on nickel beads (Novagen) were performed essentially as previously described (*13*) except complexes were formed in physiological salt buffer.

To generate purified KHC ± KLC, a bacterial lysate containing His−KHC(771−963) was first passed over a column (1 mL bed volume) of nickel beads (Novagen). The column was either washed before elution or washed before addition of a bacterial lysate containing untagged KLC (4−569). In the latter case the column was again washed prior to elution. The binding, wash, and elution conditions were as described in Novagen technical bulletin TB054. The only exception being the wash buffer contained 120 mM imidazole. Fractions containing eluted KHC or KHC/KLC were then diluted 10-fold with binding buffer used in GST pulldown experiments (phosphate-buffered saline, pH 7.2, 5 mM dithiothreitol, 0.1% (v/v) Triton X-100) prior to addition to GST-fusion proteins on glutathione sepharose beads. Beads were incubated for 2 h at 4 °C with rocking prior to washing and eluting as described above for GST pulldown experiments.

Analysis of Protein Complexes. Protein complexes were separated by SDS-PAGE and proteins identified by immunoblotting as previously described (*13*). Antibodies used included mouse monoclonal anti-KLC (L2; Chemicon Chemical Co) (*29*), and mouse monoclonal antibodies (Santa Cruz Biotechnology) against fusion tags including hemagglutinin (HA), LexA, and His.

RESULTS

Yeast Two-Hybrid Analysis of the Interaction of uKHC with SNAP25 and SNAP23. We employed a yeast two-hybrid screen using a fragment (amino acids 814−963; Figure 1A) of human uKHC as bait and a human brain cDNA library as target. As a result of this screen, 13 clones were identified which corresponded to the SNARE (soluble *N*-ethylmaleimide-sensitive attachment protein receptor) protein SNAP25, which is expressed in neurons and neuroendocrine cells (*30*)

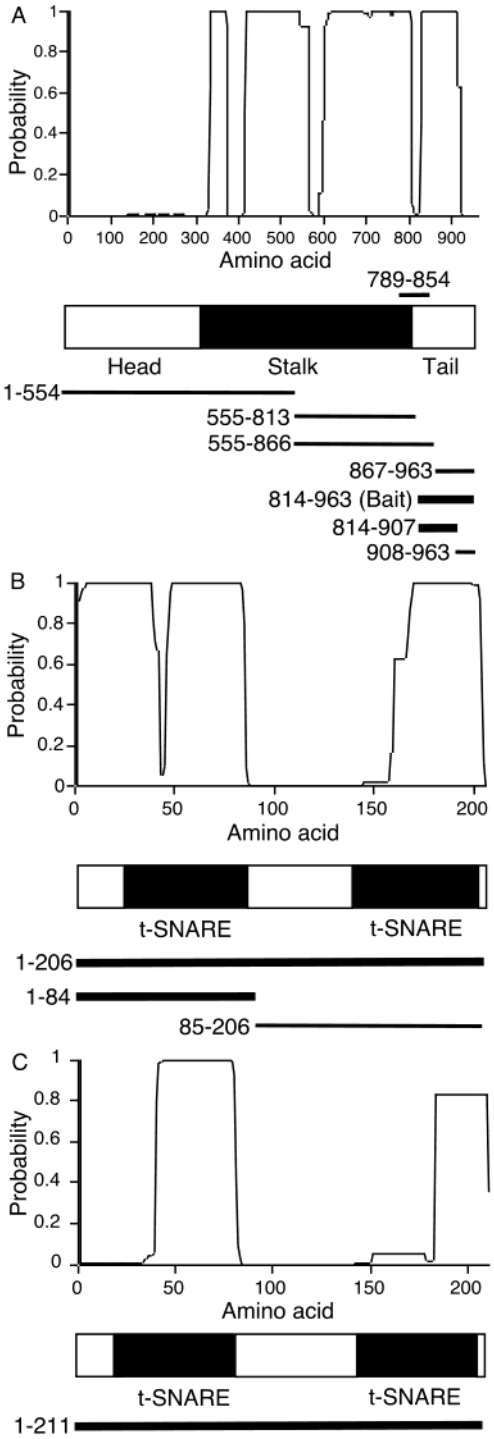

FIGURE 1: Diagram of proteins and their fragments expressed in this study. The presence of heptad repeats and therefore the probability of forming coiled-coils were determined for each protein sequence using the coils server (http://www.ch.embnet.org/software/COILS_form.html) which employs the Lupas algorithm (*54*). The MTIDK matrix with a window of 28 amino acids was employed. Domain structure is illustrated for each protein. For SNAP25 and SNAP23 proteins, the coiled-coil t-SNARE homology domain is indicated (*55*). In each case fragments illustrated with thicker lines are positive for uKHC/SNAP interaction. (A) Human uKHC showing head, stalk, and tail domains (*7*) with indicated KLC binding site (789−854) as determined in this study. (B) Human SNAP25B (*32*). (C) Human SNAP23A (*34*). Genbank accession numbers used were NM_004521 (uKHC), L19761 (SNAP25), and U55936 (SNAP23).

A

Bait/KHC Fusion	Target/SNAP Fusion	Result on -Leu/X-gal	b-Galactosidase Activity
555-813	SN25 (1-206)	No growth	3.3 ± 2.9
814-963	SN25 (1-206)	Blue growth	2041 ± 352
814-907	SN25 (1-206)	Blue growth	103 ± 21
908-963	SN25 (1-206)	No growth	9.8 ± 3.2
814-963	SN25 (1-84)	Blue growth	143 ± 25
814-963	SN25 (85-206)	No growth	9.6 ± 2.8
555-813	SN23 (1-211)	No growth	6.1 ± 3.8
814-963	SN23 (1-211)	Blue growth	310 ± 57
814-907	SN23 (1-211)	Blue growth	950 ± 166
908-963	SN23 (1-211)	No growth	11.1 ± 1.0
814-907	No insert	No growth	8.0 ± 4.4

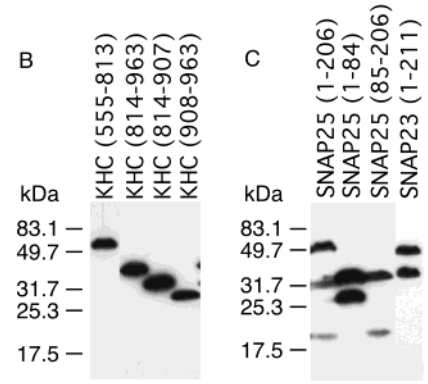

FIGURE 2: Yeast two-hybrid analysis of the interaction of uKHC with SNAP25 and SNAP23 proteins. (A) Summary of binding data obtained with yeast co-transformed with various combinations of bait/uKHC and target/SNAP25 or SNAP23 fusion constructs. Interactions were initially assessed using a qualitative in vivo plate assay with readout being expression of the reporter genes *LEU2* and *lacZ*. A true interaction was scored as blue growth. No growth indicates a negative interaction. Interactions were then quantified using a liquid β-galactosidase assay. The activity was calculated from the following equation: β-galactosidase activity $= 1000 \times A_{420}/(t \times V \times \mathrm{OD}_{660})$, where $t =$ time (in minutes) of incubation and $V =$ volume of cells (mL) used in the assay. Given activity values are the average of measurements from at least three separate colonies. (B and C) Expression of bait and target fusion proteins used in the yeast two-hybrid analysis. Protein samples were separated by SDS−PAGE (14%) prior to immunoblotting with anti-LexA (B) or anti-HA (C) antibodies.

and has a central role in synaptic vesicle exocytosis (*31*). The clones included full-length (amino acids 1−206) and various N-terminal truncations of up to eight amino acids. The isoform identified corresponded to SNAP25B (*32*), which is the dominant species in neurons (*33*).

To further define the interaction between SNAP25 and uKHC, fragments of both proteins were expressed in yeast two-hybrid vectors. Positive interactions were initially assessed by activation of both reporter genes *LEU2* and *lacZ*, resulting in blue colonies on −Leu/X-gal plates. Quantitative β-galactosidase activity was also determined. The full-length SNAP25 clone (amino acids 1−206) as isolated in the initial screen was tested for interaction with several uKHC fragments (Figure 1A). Due to the presence of noncoding SNAP25 DNA sequence upstream of the ORF, this clone had an additional amino acid sequence of AQPLPTAT at the N-terminus of SNAP25 in frame with the activation domain tag. SNAP25(1−206) interacted with the original bait uKHC(814−963) and with uKHC(814−907) but not with uKHC(555−813) or uKHC(908−963) (Figure 2A). The fragment uKHC(1−554) in displayBAIT vector was also constructed but could not be analyzed in the yeast two-hybrid assay since it was found to autoactivate the reporter genes (data not shown). From β-galactosidase activity measurements, the strength of the interaction of SNAP25 with uKHC-(814−907) is significantly weaker than that with uKHC-(814−963) (Figure 2A). As there appears to be no direct interaction with uKHC(908−963), it is likely that the minimal binding domain is within uKHC(814−907). Differences in binding were not due to differences in proteins expressions levels of the bait/uKHC fusion proteins (Figure 2B).

Known homologues of SNAP25 include SNAP23 (*34*) and syndet (*35*), both of which most likely substitute for SNAP25 in nonneuronal cells. SNAP23 was also tested for interaction with uKHC on the basis that the SNAP25-uKHC interaction is important in all cell types. To date, five splice variants of SNAP23 have been identified (*36*, *37*). Full-length variant SNAP23A used in this study has 59% homology and 72% similarity to SNAP25B at the amino acid level (Figure 3) (*34*). SNAP25B itself differs from SNAP25A by only nine amino acids as a result of alternative splicing (Figure 3) (*32*). The interaction pattern of full-length SNAP23 (amino acids 1−211) with uKHC fragments was similar to that of SNAP25 (Figure 2A), and like SNAP25, the minimal interacting kinesin fragment was uKHC(814−907). In contrast to SNAP25, though, SNAP23 was found to interact with fragment 814−907 to a greater degree than with 814−963. Even with this variability in activity measurements the fact remains that both SNAP25 and SNAP23 binding maps to residues 814−907 of uKHC. This region has been shown to interact with other postulated cargo proteins including kinectin (*24*) and US11 (*26*). Expression of target/SNAP25 and SNAP23 fusion proteins were similar (Figure 2C). In addition, the interaction between uKHC(814−963) and SNAP25 or SNAP23 was confirmed to work equally well in reverse using bait/SNAP and target/KHC yeast two-hybrid constructs (result not shown).

Two fragments of SNAP25, amino acids 1−84 and 85−206, were then generated to ascertain which region was important for interaction with uKHC. Fragment 1−84 spans the first two heptad-repeat regions and the first target membrane (t)-SNARE domain (Figure 1B). Fragment 85−206 spans a nonheptad repeat region, containing four cysteine residues (positions 85, 88, 90, and 92) which are palmitoylated for membrane association (*38*), along with the C-terminal heptad repeat t-SNARE domain (Figure 1B). Analysis by yeast two-hybrid assay revealed that uKHC-(814−963) interacts only with SNAP25(1−84), though with a lower affinity than with SNAP25(1−206), and not with SNAP25(85−206) (Figure 2A). Expression of target-SNAP25-(1−206) and fragments were similar (Figure 2C). The equivalent region (1−79) in SNAP23, though similar in sequence (Figure 3), does not contain the most N-terminal heptad-repeat region (Figure 1C). This suggests that the uKHC-binding region within SNAP23 and SNAP25 lies in the common heptad-repeat domain between residues 45−84 in SNAP25 and residues 40−79 in SNAP23 (Figure 3). Note that the N-terminal t-SNARE domain, present in both SNAP25 (residues 19−81) and SNAP23 (residues 14−76), incorporates the majority of this heptad-repeat region. Syndet, which is more closely related to SNAP23 (86% homology) than to SNAP25, also lacks this N-terminal heptad-repeat

```
                                                                cdefgabcdefgabcd
hsSNAP25A   MAEDADMRNELEEMQRRADQLADESLESTRRMLQLVEESKDAGIRTLVMLDEQGEQLDRV 60
hsSNAP25B   MAEDADMRNELEEMQRRADQLADESLESTRRMLQLVEESKDAGIRTLVMLDEQGEQLERI 60
hsSNAP23A   -MDNLSS----EEIQQRAHQITDESLESTRRILGLAIESQDAGIKTITMLDEQKEQLNRI 55
              :: .     **:*:**.*::*********:* *. **:****:*:.***** ***:*:
            efgabcdefgabcdefgabcdefg
hsSNAP25A   EEGMNHINQDMKEAEKNLKDLGKCCGLFICPCNKLK---SSDAYKKAWGNNQDG----VV 113
hsSNAP25B   EEGMDQINKDMKEAEKNLTDLGKFCGLCVCPCNKLK---SSDAYKKAWGNNQDG----VV 113
hsSNAP23A   EEGLDQINKDMRETEKTLTELNKCCGLCVCPCNRTKNFESGKAYKTTWGDGGENSPCNVV 115
            ***:::**:**:*:**.*.:*.* *** :****: *   *..***.:**:. :.    **

hsSNAP25A   ASQPARVVDEREQM----AISGGFIRRVTNDARENEMDENLEQVSGIIGNLRHMALDMGN 169
hsSNAP25B   ASQPARVVDEREQM----AISGGFIRRVTNDARENEMDENLEQVSGIIGNLRHMALDMGN 169
hsSNAP23A   SKQPGPVTNGQLQQPTTGAVSGGYIKRITNDAREDEMEENLTQVGSILGNLKDMALNIGN 175
            :.**. *.: : *     *:***:*:*:******:**:*** **..*:***:.***::**

hsSNAP25A   EIDTQNRQIDRIMEKADSNKTRIDEANQRATKMLGSG 206
hsSNAP25B   EIDTQNRQIDRIMEKADSNKTRIDEANQRATKMLGSG 206
hsSNAP23A   EIDAQNPQIKRITDKADTNRDRIDIANARAKKLIDS- 211
            ***:** **.** :***:*: *** ** **.*::.*
```

FIGURE 3: Protein sequence alignment of human SNAP25A, SNAP25B, and SNAP23A. Alignments were generated using the Clustalw program (*56*) at http://www2.ebi.ac.uk/clustalw. Gaps are introduced to maximize the alignment with identical residues (*), conservative substitutions (**:**), and semiconservative substitutions (**.**) indicated. The region of difference between SNAP25A and SNAP25B occurs between the arrows with the amino acid changes indicated (●). The proposed binding site for uKHC is indicated by the boxed region with the heptad-repeat sequence labeled as *abcdefg*. Genbank accession number used for SNAP25A was L19760 (*32*).

region but, like SNAP23 and SNAP25, contains the other two heptad-repeat regions (*35*).

*In Vitro Analysis of the Interaction of uKHC with SNAP25 and SNAP2*3. The interaction of uKHC with SNAP25 and SNAP23 was confirmed using an in vitro pulldown assay. His-tagged fragments spanning the entire uKHC protein sequence were analyzed for interaction with GST-tagged fusions of SNAP25(1−206), SNAP25(1−84) and SNAP25-(85−206). These SNAP25 constructs were generated without the additional N-terminal sequence AQPLPTAT present in the yeast two-hybrid constructs. In agreement with the yeast two-hybrid analysis, only uKHC(814−963) was found to bind to SNAP25(1−206) (Figure 4A). In further agreement, only SNAP25(1−84) and not SNAP25(85−206) bound to uKHC(814−963) (Figure 4A). All GST−SNAP25 fusion proteins were confirmed to be present at similar levels in the pulldown assay (Figure 4B). It is of interest to note that the uKHC(814−963) present in pull-downs with GST−SNAP25 has a lower molecular weight band (Figure 4A). This band appears to be enriched in the pull-downs and represents a fragment derived from His−KHC(814−963) since the band is not present in any other KHC pull-downs or bacterial lysates. In addition it must be a C-terminal truncation as the His tag, which is the basis of detection in the assay, is at the N-terminus of uKHC. The proteolytic fragment is approximately 3 kDa smaller than His−KHC-(814−963) and would represent the loss of at least half of the 6 kDa nonheptad repeat tail region (residues 908−963). Though not directly tested in this assay, it does add support to the yeast two-hybrid finding that at least some or all of this region is not directly involved in binding SNAP25 or SNAP23.

The same His-tagged uKHC fragments were analyzed for interaction with GST-tagged SNAP23(1−211). Again, in agreement with the yeast two-hybrid analysis, only uKHC-(814−963) was found to bind to GST−SNAP23 with no binding to GST only (Figure 5A). Both GST and GST−SNAP23 fusion proteins were confirmed to be present in the pulldown assay (Figure 5B). There was also a proteolytic

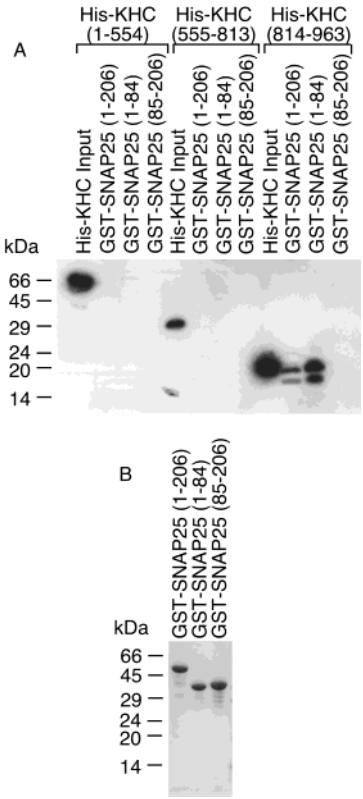

FIGURE 4: In vitro binding of uKHC and SNAP25. Complexes of His−KHC and GST−SNAP25 were eluted from glutathione sepharose beads and separated by SDS-PAGE (14%). (A) Immunoblot with anti-His tag antibody. Expression of each input His−KHC fragment was confirmed in bacterial lysates. (B) Coomassie blue staining to confirm the presence of GST−SNAP25 proteins in the in vitro pulldown assay.

fragment of uKHC(814−963) in the pulldown with GST−SNAP23 (Figure 5A).

In Vitro Analysis of the Interaction of KLC and SNAP25. An in vitro pulldown assay was initially used to determine if KLC directly bound to SNAP25. Untagged KLC was analyzed for interaction with GST-tagged uKHC(555−963),

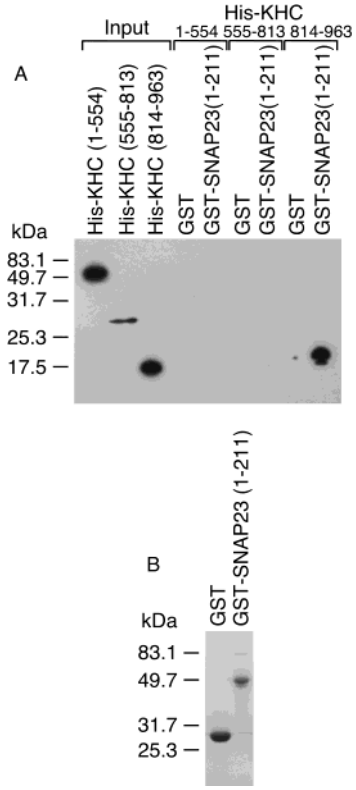

FIGURE 5: In vitro binding of uKHC and SNAP23. Complexes of His−KHC and GST−SNAP23 were eluted from glutathione sepharose beads and separated by SDS-PAGE (14%). (A) Immunoblot with anti-His tag antibody. Expression of each input His−KHC fragment was confirmed in bacterial lysates. (B) Coomassie blue staining to confirm the presence of GST and GST−SNAP23 proteins in the in vitro pulldown assay.

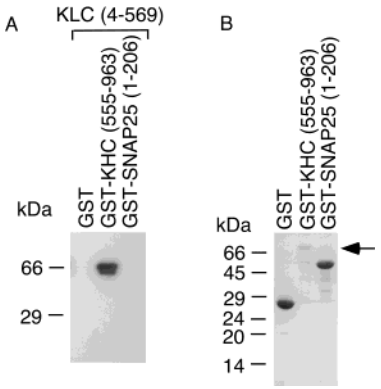

FIGURE 6: In vitro binding analysis of the interaction of KLC with uKHC and SNAP25. Complexes of untagged KLC and GST fusion proteins were eluted from glutathione sepharose beads and separated by SDS-PAGE (14%). (A) Immunoblot with anti-KLC antibody. (B) Coomassie blue staining to confirm the presence of GST and GST-fusion proteins in the in vitro pulldown assay. The position of GST−KHC(555−963), which is present at low levels, is indicated by an arrow.

a heavy-chain fragment which contains the known KLC-interaction site (*12*, *13*), and GST-tagged SNAP25(1−206). KLC was found to bind to the positive control, GST−KHC, but did not bind to either GST or GST−SNAP25 (Figure 6A). Both GST and GST−SNAP25 fusion proteins were confirmed to be present at similar levels in the pulldown assay (Figure 6B). GST−KHC was present in quite low amounts but still strongly bound KLC (Figure 6B).

Analysis of the Interaction of KLC, SNAP25, SNAP23, and uKHC. The fragments KLC(1−199) and KLC(200−569) in displayBAIT vector were constructed to verify the in vitro pulldown binding results obtained with KLC and SNAP25. Both KLC bait vector constructs were found to autoactivate the reporter genes (data not shown), so they were subsequently inserted into displayTARGET while SNAP25 and SNAP23 were inserted into displayBAIT. Analysis of binding using the yeast two-hybrid assay revealed, in agreement with the in vitro pulldown assay, that neither KLC fragment binds to SNAP25 or SNAP23 (Figure 7A). In particular, the known cargo-binding TPR domain of KLC (*14*), contained within fragment 200−569, did not bind to either SNAP protein. Expression of bait/SNAP (Figure 7B) and target/KLC (Figure 7C) fusion proteins were also verified.

In an attempt to clearly ascertain whether the binding sites for KLC and SNAP proteins in uKHC are distinct or overlap, uKHC fragments in bait were tested against KLC fragments, full-length SNAP25 or SNAP23 in target. The positive control included in this experiment consisted of uKHC(555−813) and KLC(4−199) which contain the known heavy and light chain interacting sites (*12*, *13*). As expected, this combination interacts in the yeast two-hybrid assay (Figure 7A). Somewhat unexpectedly, the combination of uKHC-(814−963) and KLC(4−199) also gave blue colonies on selective media. Subsequent measurement of β-galactosidase activity for this interaction showed that it was not above background (taken as values obtained for no growth combinations), suggesting that it is a very weak interaction (Figure 7A). Further analysis with uKHC(555−866) showed the relative strength of binding of KLC(4−199) to be greatest with this fragment, with no binding to uKHC(867−963) (Figure 7A). Expression of uKHC(555−866) and uKHC-(867−963) in bait was also verified and found to be similar (Figure 7B).

Our previous studies on the uKHC/KLC interaction were based on an in vitro pulldown assay using C-terminal truncations of uKHC (*13*). Deletion of region 814−963 had relatively little effect on KLC binding, but the region was never directly tested for binding of uKHC. A uKHC fragment spanning region 855−963 was tested though and found not to bind KLC. Therefore, to verify the yeast two-hybrid analysis, we tested an additional range of His-tagged uKHC fragments for binding of KLC using an in vitro pulldown assay (Figure 7D). The presence of each His−KHC fragment in the pulldown assay was confirmed by staining with coomassie blue (result not shown). The interactions of KLC with uKHC fragments 771−876, 555−813, and 789−963 were positive (Figure 7D, top panel). Only on overexposure of the blot was there any binding detected with uKHC fragment 814−963 (Figure 7D, bottom panel). This confirms the yeast two-hybrid analysis indicating that KLC does bind to uKHC(814−963), though significantly weaker than to uKHC(555−813). Furthermore, the fact that KLC binds to uKHC fragment 789−963 and not to 555−788 further defines the major KLC-binding site in uKHC from region 771−813 (*13*) to 789−813. An apparent minor KLC-binding site occurs between uKHC residues 814 and 854, which span the N-terminus of the tail domain and overlap with the predicted cargo-binding domain (814−907) (Figure 1A). This is in fact in agreement with previous work which suggested that KLC binding to uKHC was dependent not only on the

A

Bait Fusion	Target Fusion	Result on −Leu/X-gal	b-Galactosidase Activity*
SN25(1-206)	KLC(4-199)	No growth	0.9 ± 0.6
SN25(1-206)	KLC(200-569)	No growth	13.1 ± 1.8
SN23(1-211)	KLC(4-199)	No growth	0.7 ± 0.5
SN23(1-211)	KLC(200-569)	No growth	7.0 ± 3.1
KHC(555-813)	KLC(4-199)	Blue growth	212 ± 19
KHC(555-813)	KLC(200-569)	No growth	ND
KHC(814-963)	KLC(4-199)	Blue growth	9 ± 4
KHC(814-963)	KLC(200-569)	No growth	ND
KHC(555-866)	KLC(4-199)	Blue growth	551 ± 70
KHC(555-866)	KLC(200-569)	No growth	ND
KHC(867-963)	KLC(4-199)	No growth	ND
KHC(867-963)	KLC(200-569)	No growth	ND
KHC(555-866)	SN25(1-206)	No growth	ND
KHC(555-866)	SN25(1-206)	No growth	ND
KHC(867-963)	SN23(1-211)	No growth	ND
KHC(867-963)	SN23(1-211)	No growth	ND

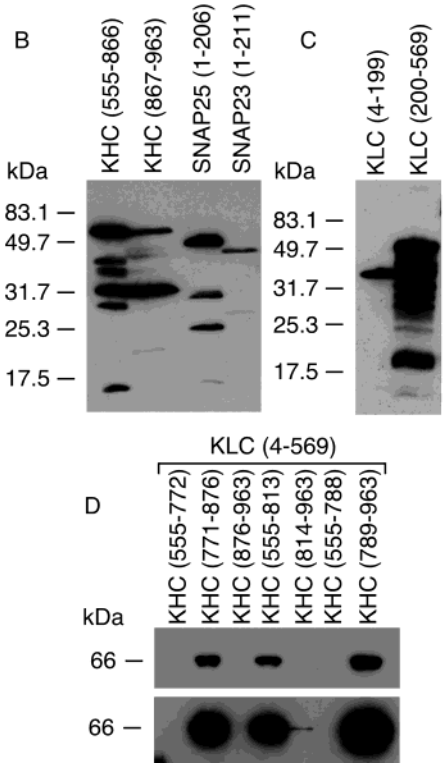

FIGURE 7: Analysis of the interaction of KLC, SNAP25, SNAP23, and uKHC proteins. (A) Yeast two-hybrid analysis showing summary of binding data obtained with yeast co-transformed with various combinations of bait/SNAP25, SNAP23, or uKHC fusion constructs and target/SNAP25, SNAP23, or KLC fusion constructs. Interactions were initially assessed using a qualitative in vivo plate assay with readout being expression of the reporter genes *LEU2* and *lacZ*. A true interaction was scored as blue growth. No growth indicates a negative interaction. Interactions were then quantified using a liquid β-galactosidase assay. The activity was calculated from the following equation: β-galactosidase activity $= 1000 \times A_{420}/(t \times V \times OD_{660})$, where $t =$ time (in minutes) of incubation and $V =$ volume of cells (mL) used in the assay. Given activity values are the average of measurements from at least three separate colonies. ND, not determined. (B and C) Expression of bait and target fusion proteins used in the yeast two-hybrid analysis. Protein samples were separated by SDS-PAGE (14%) prior to immunoblotting with anti-LexA (B) or anti-HA (C) antibodies. (D) In vitro binding of uKHC and KLC. Complexes of His−KHC and untagged KLC were eluted from nickel beads and separated by SDS-PAGE (14%) before immunoblotting with anti-KLC antibody. Top and bottom panels are identical blots with differing exposure times.

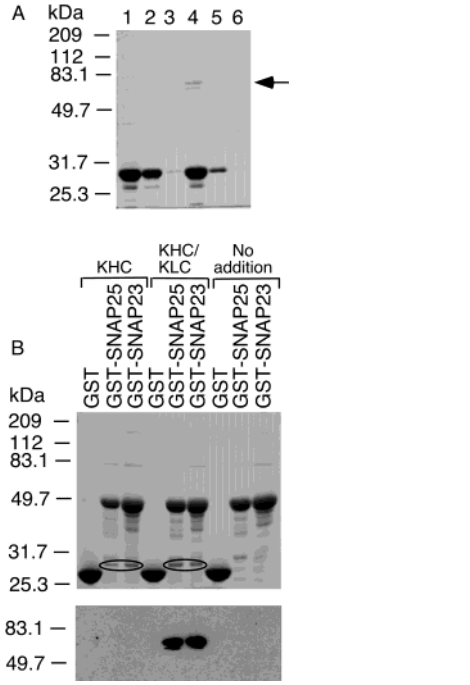

FIGURE 8: In vitro binding of SNAP25 and SNAP23 to a complex of uKHC/KLC. Proteins were separated by SDS-PAGE (12%). (A) Purification of KHC and KHC/KLC from nickel beads. Coomassie blue staining of eluted fractions containing either His−KHC(771−963) alone (lanes 1−3) or a complex of His−KHC(771−963) and untagged KLC (indicated by an arrow; lanes 4−6). (B) Binding of purified KHC and KHC/KLC to GST−SNAP25(1−206) and GST−SNAP23(1−211). Coomassie blue staining (upper panel) shows His−KHC(771−963) (indicated by a circle) coeluting with both GST−SNAP proteins (uppermost bands) in the absence or presence of KLC. In the lower panel, the same samples were immunoblotted with anti-KLC antibody.

C-terminal end of the KHC stalk domain but also on the N-terminal end of the KHC tail domain (*12*). We have also shown that the TPR-containing KLC fragment 200−569 does not appear to directly bind to uKHC, at least not to region 555−963 (Figure 7A).

Surprisingly, neither uKHC fragment 555−866 or 867−963 was found to bind to SNAP25 or SNAP23 (Figure 7A). This suggests that the heptad repeat region within uKHC fragment 814−907 responsible for binding of SNAP proteins is located either side of positions 866/867 and cutting at this position abolishes binding of SNAP proteins. This contrasts with our findings with herpes simplex viral protein US11 which interacts only with region 867−894 of uKHC (*26*).

To add weight to the argument that the observed KHC/SNAP interaction has an in vivo role, we looked at the binding of SNAP proteins to a performed complex of kinesin heavy and light chain. A His−KHC fragment spanning amino acids 771−963 (contains both KLC and SNAP binding sites) was purified on nickel beads with or without untagged KLC(4−569) (Figure 8A). All the coeluting KLC must be present in a complex with KHC, as it does not directly bind to the His tag or to nickel beads (Figure 7D). The amount of KHC containing bound KLC was <5 wt % (Figure 8A, lane 4) but deemed sufficient to determine qualitatively if the KHC/KLC complex could bind to SNAP proteins. Approximately 100 ug of His−KHC(771−963) ± KLC(4−569) was then added to GST−SNAP proteins. Eluted complexes showed that equivalent amounts of His−KHC ± KLC coeluted with both SNAP25 and SNAP23 with

no binding to GST alone (Figure 8B, upper panel). KLC when added as part of a complex with KHC also coeluted with both SNAP25 and SNAP23 with no binding to GST alone (Figure 8B, lower panel). On the basis that KLC does not directly bind to SNAP proteins (Figures 6A and 7A) and the His tag does not bind to GST−SNAP proteins on glutathione sepaharose beads (Figures 4A and 5A) then the presence of KLC indicates that SNAP proteins can bind to a complex of kinesin heavy and light chain. This shows qualitatively that the KLC and SNAP proteins do not compete for the same binding site on KHC and as such supports an in vivo role for the observed KHC/SNAP interaction. Whether KLC directly or indirectly influences binding of KHC to SNAP proteins requires further evaluation. Clearly, though, KHC can bind to SNAP in the absence of KLC, and SNAP proteins do not directly bind to KLC, at least in the absence of KHC. This suggests any role KLC may have would likely be to regulate the interaction of KHC with SNAP.

Yeast Two-hybrid Analysis of the Interaction of SNAP25 and SNAP23 with Subunits of other Motor Proteins. To confirm the specificity of the identified interaction of uKHC with SNAP25 and SNAP23, the same SNAP proteins were tested for interactions with several subunits of the retrograde motor dynein and an accessory subunit of kinesin KIF3. Subunits of dynein known to have a role in cargo binding were chosen and included DLCs LC8 (*39*), RP3 and TcTex1 (*40*), along with DIC-1c (*28*). The known interactions between DIC and DLCs were all confirmed in our yeast two-hybrid assay and included DIC-LC8 in both directions, DIC with each DLC and dimerization of LC8 (*40*, *41*) (Figure 9A). No interactions were observed between any tested dynein subunits and SNAP25 or SNAP23 (Figure 9A). This is not unexpected, as SNAP25 appears to undergo limited retrograde transport as it is degraded at the axon termini (*42*). The accessory cargo-binding subunit (KAP3B) of another kinesin, KIF3, known to play a role in anterograde axonal transport of membranous organelles (*43*), was also found not to interact with either SNAP25 or SNAP23 (Figure 9A). Expression of all dynein subunits and KAP3B was also verified (Figure 9B and C). These findings validate both the yeast two-hybrid assay and the specificity of the identified uKHC/SNAP interaction.

A

Bait Fusion	Target Fusion	Result on −Leu/X-gal	β-Galactosidase Activity*
DIC	DIC	No growth	5.7 ± 3.1
DIC	LC8	Blue growth	1304 ± 561
DIC	RP3	Blue growth	798 ± 127
DIC	TcTex1	Blue growth	1651 ± 180
No insert	LC8	No growth	3.0 ± 2.8
LC8	DIC	Blue growth	396 ± 110
LC8	LC8	Blue growth	871 ± 47
LC8	RP3	No growth	10.5 ± 2.1
LC8	TcTex1	No growth	8.5 ± 2.1
DIC	SN25(1-206)	No growth	ND
LC8	SN25(1-206)	No growth	ND
DIC	SN23(1-211)	No growth	ND
LC8	SN23(1-211)	No growth	ND
SN25(1-206)	TcTex1	No growth	ND
SN25(1-206)	RP3	No growth	ND
SN25(1-206)	KAP3B	No growth	ND
SN23(1-211)	TcTex1	No growth	ND
SN23(1-211)	RP3	No growth	ND
SN23(1-211)	KAP3B	No growth	ND

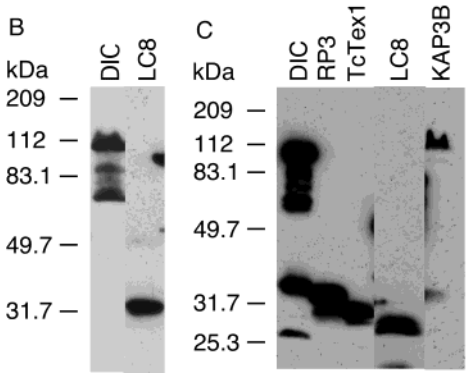

FIGURE 9: Yeast two-hybrid analysis of the interaction of SNAP25 and SNAP23 with subunits of other motor proteins. (A) Summary of binding data obtained with yeast co-transformed with various combinations of bait/SNAP25, SNAP23, or dynein fusion constructs and target/SNAP25, SNAP23, dynein, or KAP3B fusion constructs. Interactions were initially assessed using a qualitative in vivo plate assay with readout being expression of the reporter genes *LEU2* and *lacZ*. A true interaction was scored as blue growth. No growth indicates a negative interaction. Interactions were then quantified using a liquid β-galactosidase assay. The activity was calculated from the following equation: β-galactosidase activity $= 1000 \times A_{420}/(t \times V \times OD_{660})$, where $t =$ time (in minutes) of incubation and $V =$ volume of cells (mL) used in the assay. Given activity values are the average of measurements from at least three separate colonies. ND, not determined. (B and C) Expression of bait and target fusion proteins used in the yeast two-hybrid analysis. Protein samples were separated by SDS-PAGE (12%) prior to immunoblotting with anti-LexA (B) or anti-HA (C) antibodies.

DISCUSSION

The process of regulated exocytosis in neurons to release neurotransmitters requires specific protein−protein interactions to fuse the synaptic vesicle with the plasma membrane at the nerve terminal. The fusion or SNARE complex results from the interaction of the t-SNARE proteins, SNAP25, and syntaxin, which form a receptor complex on the plasma membrane for the vesicle membrane−SNARE protein, VAMP (vesicle-associated membrane protein; also termed synaptobrevin) (*31*). Both VAMP and syntaxin have carboxy-terminal transmembrane domains, while SNAP25 is held to the membrane by palmitoylation.

The concept that different classes of transport organelles or vesicles containing different membrane proteins are sorted in the cell body and transported by specific motors has been previously proposed (*44*). This was based on the finding that the KIF1A kinesin was found to be associated with organelles containing synaptic vesicle proteins such as synaptotagmin, synatophysin, and Rab3A. These KIF1A-associated vesicles did not contain syntaxin 1A or SNAP25. In addition, the same vesicles were not associated with conventional kinesin or KIF3. The demonstration in this study that conventional uKHC interacts directly with the presynaptic membrane t-SNARE protein SNAP25 supports this model of specific motor proteins transporting different classes of organelles along axons. The importance of this interaction in vivo is yet to be demonstrated but a number of studies do support a biological role for the interaction. The transport of synaptic vesicles and membranes containing presynaptic membrane

proteins along axons from the cell body to the nerve termini occurs at a rate indicative of kinesin-dependent fast anterograde transport (*42*, *45*−*48*). A direct in vivo role for conventional kinesin in transport of vesicles during regulated exocytosis has been demonstrated (*23*). In addition, conventional kinesin immunoreactivity colocalizes in axons with VAMP1 and SNAP25 (*45*).

The nature of the complex formed between SNAP25, VAMP, and syntaxin is dependent on heptad-repeat regions in each protein which form a trimeric α-helical coiled-coil (*49*, *50*). The nature of the uKHC−SNAP25 interaction is also dependent on heptad-repeat regions in each protein. The predicted cargo-binding domain of uKHC (residues 814−907) was confirmed as the binding site for the amino-terminal half of SNAP25. The amino-terminal half of SNAP25 interacts with syntaxin, while both the second and third heptad-repeats regions of SNAP25 (Figure 1B) are necessary for interaction with VAMP (*49*, *50*).

It has been proposed that components of the nerve terminal, including synaptic vesicles and membranes containing presynaptic membrane proteins, are either transported separately or are pre-assembled in the cell body prior to kinesin-dependent transport down axons (*51*). A number of studies have shown that VAMP, syntaxin, and SNAP25 are associated during axonal transport (*42*, *46*, *52*) and an assembled presynaptic complex is transported down axons (*47*). It is tempting to speculate that the uKHC−SNAP25 interaction identified in this study is important for transport of these pre-assembled complexes. SNAP25 may be the only link or other proteins in the complex may well bind to motor proteins. To address these issues, it would be worth testing whether VAMP and syntaxin can directly bind to uKHC and whether uKHC can bind to a complex of SNAP25, VAMP, and syntaxin.

The uKHC−SNAP25 interaction is also most likely important in all cells as the ubiquitously expressed SNAP25 homologue, SNAP23, was also shown to interact with uKHC. This would suggest that conventional kinesin also transports SNAP23-containing vesicles, probably in a complex with ubiquitously expressed isoforms of syntaxin and VAMP which interact with SNAP23 (*53*), to the plasma membrane to mediate constitutive exocytosis.

REFERENCES

1. Goldstein, L. S., and Yang, Z. (2000) *Annu. Rev. Neurosci. 23*, 39−71.
2. Hirokawa, N. (1998) *Science 279*, 519−526.
3. Brady, S. T. (1985) *Nature 317*, 73−75.
4. Vale, R. D., Reese, T. S., and Sheetz, M. P. (1985) *Cell 42*, 39−50.
5. Bloom, G. S., Wagner, M. C., Pfister, K. K., and Brady, S. T. (1988) *Biochemistry 27*, 3409−3416.
6. Xia, C., Rahman, A., Yang, Z., and Goldstein, L. S. (1998) *Genomics 52*, 209−213.
7. Navone, F., Niclas, J., Hom-Booher, N., Sparks, L., Bernstein, H. D., McCaffrey, G., and Vale, R. D. (1992) *J. Cell Biol. 117*, 1263−1275.
8. Niclas, J., Navone, F., Hom-Booher, N., and Vale, R. D. (1994) *Neuron 12*, 1059−1072.
9. Nakagawa, T., Tanaka, Y., Matsuoka, E., Kondo, S., Okada, Y., Noda, Y., Kanai, Y., and Hirokawa, N. (1997) *Proc. Natl. Acad. Sci. U.S.A. 94*, 9654−9659.
10. Rahman, A., Friedman, D. S., and Goldstein, L. S. (1998) *J. Biol. Chem. 273*, 15395−15403.
11. Gauger, A. K., and Goldstein, L. S. (1993) *J. Biol. Chem. 268*, 13657−13666.
12. Verhey, K. J., Lizotte, D. L., Abramson, T., Barenboim, L., Schnapp, B. J., and Rapoport, T. A. (1998) *J. Cell Biol. 143*, 1053−1066.
13. Diefenbach, R. J., Mackay, J. P., Armati, P. J., and Cunningham, A. L. (1998) *Biochemistry 37*, 16663−16670.
14. Gindhart, J. G., Jr., and Goldstein, L. S. (1996) *Trends Biochem. Sci. 21*, 52−53.
15. Verhey, K. J., Meyer, D., Deehan, R., Blenis, J., Schnapp, B. J., Rapoport, T. A., and Margolis, B. (2001) *J. Cell Biol. 152*, 959−970.
16. Bowman, A. B., Kamal, A., Ritchings, B. W., Philp, A. V., McGrail, M., Gindhart, J. G., and Goldstein, L. S. (2000) *Cell 103*, 583−594.
17. Kamal, A., Almenar-Queralt, A., LeBlanc, J. F., Roberts, E. A., and Goldstein, L. S. (2001) *Nature 414*, 643−648.
18. Kamal, A., Stokin, G. B., Yang, Z., Xia, C. H., and Goldstein, L. S. (2001) *Neuron 28*, 449−459.
19. Rietdorf, J., Ploubidou, A., Reckmann, I., Holmstrom, A., Frischknecht, F., Zettl, M., Zimmermann, T., and Way, M. (2001) *Nat. Cell Biol. 3*, 992−1000.
20. Kirchner, J., Seiler, S., Fuchs, S., and Schliwa, M. (1999) *Embo J. 18*, 4404−4413.
21. Seiler, S., Kirchner, J., Horn, C., Kallipolitou, A., Woehlke, G., and Schliwa, M. (2000) *Nat. Cell Biol. 2*, 333−338.
22. Skoufias, D. A., Cole, D. G., Wedaman, K. P., and Scholey, J. M. (1994) *J. Biol. Chem. 269*, 1477−1485.
23. Bi, G. Q., Morris, R. L., Liao, G., Alderton, J. M., Scholey, J. M., and Steinhardt, R. A. (1997) *J. Cell Biol. 138*, 999−1008.
24. Ong, L. L., Lim, A. P., Er, C. P., Kuznetsov, S. A., and Yu, H. (2000) *J. Biol. Chem. 275*, 32854−32860.
25. Cai, Y., Singh, B. B., Aslanukov, A., Zhao, H., and Ferreira, P. A. (2001) *J. Biol. Chem. 276*, 41594−41602.
26. Diefenbach, R. J., Miranda-Saksena, M., Diefenbach, E., Holland, D. J., Boadle, R. A., Armati, P. J., and Cunningham, A. L. (2002) *J. Virol. 76*, 3282−3291.
27. Valdez, A. C., Cabaniols, J. P., Brown, M. J., and Roche, P. A. (1999) *J. Cell Sci. 112*, 845−854.
28. Crackower, M. A., Sinasac, D. S., Xia, J., Motoyama, J., Prochazka, M., Rommens, J. M., Scherer, S. W., and Tsui, L. C. (1999) *Genomics 55*, 257−267.
29. Pfister, K. K., Wagner, M. C., Stenoien, D. L., Brady, S. T., and Bloom, G. S. (1989) *J. Cell Biol. 108*, 1453−1463.
30. Oyler, G. A., Higgins, G. A., Hart, R. A., Battenberg, E., Billingsley, M., Bloom, F. E., and Wilson, M. C. (1989) *J. Cell Biol. 109*, 3039−3052.
31. Lin, R. C., and Scheller, R. H. (2000) *Annu. Rev. Cell Dev. Biol. 16*, 19−49.
32. Bark, I. C., and Wilson, M. C. (1994) *Gene 139*, 291−292.
33. Bark, I. C., Hahn, K. M., Ryabinin, A. E., and Wilson, M. C. (1995) *Proc. Natl. Acad. Sci. U.S.A. 92*, 1510−1514.
34. Ravichandran, V., Chawla, A., and Roche, P. A. (1996) *J. Biol. Chem. 271*, 13300−13303.
35. Wang, G., Witkin, J. W., Hao, G., Bankaitis, V. A., Scherer, P. E., and Baldini, G. (1997) *J. Cell Sci. 110*, 505−513.
36. Mollinedo, F., and Lazo, P. A. (1997) *Biochem. Biophys. Res. Commun. 231*, 808−812.
37. Shukla, A., Corydon, T. J., Nielsen, S., Hoffmann, H. J., and Dahl, R. (2001) *Biochem. Biophys. Res. Commun. 285*, 320−327.
38. Lane, S. R., and Liu, Y. (1997) *J. Neurochem. 69*, 1864−1869.
39. Wilson, M. J., Salata, M. W., Susalka, S. J., and Pfister, K. K. (2001) *Cell Motil. Cytoskeleton 49*, 229−240.
40. King, S. M., Barbarese, E., Dillman, J. F., 3rd, Benashski, S. E., Do, K. T., Patel-King, R. S., and Pfister, K. K. (1998) *Biochemistry 37*, 15033−15041.
41. Makokha, M., Hare, M., Li, M., Hays, T., and Barbar, E. (2002) *Biochemistry 41*, 4302−4311.
42. Li, J. Y., Jahn, R., and Dahlstrom, A. (1996) *Eur. J. Cell Biol. 70*, 12−22.
43. Takeda, S., Yamazaki, H., Seog, D. H., Kanai, Y., Terada, S., and Hirokawa, N. (2000) *J. Cell Biol. 148*, 1255−1265.
44. Okada, Y., Yamazaki, H., Sekine-Aizawa, Y., and Hirokawa, N. (1995) *Cell 81*, 769−780.
45. Li, J. Y., Pfister, K. K., Brady, S., and Dahlstrom, A. (1999) *J. Neurosci. Res. 58*, 226−241.

46. Shiff, G., and Morel, N. (1997) *J. Neurochem. 68*, 1663−1667.
47. Ahmari, S. E., Buchanan, J., and Smith, S. J. (2000) *Nat. Neurosci. 3*, 445−451.
48. Nakata, T., Terada, S., and Hirokawa, N. (1998) *J. Cell Biol. 140*, 659−674.
49. Canaves, J. M., and Montal, M. (1998) *J. Biol. Chem. 273*, 34214−34221.
50. Chapman, E. R., An, S., Barton, N., and Jahn, R. (1994) *J. Biol. Chem. 269*, 27427−27432.
51. Roos, J., and Kelly, R. B. (2000) *Nat. Neurosci. 3*, 415−417.
52. Shiff, G., and Morel, N. (1997) *J. Neurosci. Res. 48*, 313−323.
53. Foster, L. J., Yeung, B., Mohtashami, M., Ross, K., Trimble, W. S., and Klip, A. (1998) *Biochemistry 37*, 11089−11096.
54. Lupas, A., Van Dyke, M., and Stock, J. (1991) *Science 252*, 1162−1164.
55. Weimbs, T., Low, S. H., Chapin, S. J., Mostov, K. E., Bucher, P., and Hofmann, K. (1997) *Proc. Natl. Acad. Sci. U.S.A. 94*, 3046−3051.
56. Thompson, J. D., Higgins, D. G., and Gibson, T. J. (1994) *Nuc. Acids Res. 22*, 4673−4680.

BI026417U